Journal of Food Engineering 125 (2014) 44–50

Contents lists available at ScienceDirect

Journal of Food Engineering

journal homepage: www.elsevier.com/locate/jfoodeng

Proton mobility for the description of dynamic aspects of freeze-dried fruits

Lina M. Agudelo-Laverde, Carolina Schebor, María del Pilar Buera *

Departamento de Industrias, Facultad de Ciencias Exactas y Naturales, Universidad de Buenos Aires (FCEyN-UBA), Buenos Aires, Argentina

ARTICLE INFO

Article history:
Received 14 August 2013
Received in revised form 11 October 2013
Accepted 20 October 2013
Available online 26 October 2013

Keywords:
Water sorption isotherms
GAB
Generalized D'Arcy and Watt equation
Freeze-dried
Low field ^{1}H NMR

ABSTRACT

The partitioning of water sorption isotherms into different zones, according to the strength of water interactions with solids has very important practical applications. However, the dynamic properties of water play an important role in complementing the information provided by water sorption isotherms. One of the most successful techniques used to prove the dynamic behavior of water in foods systems is pulsed NMR. The aim of this study was to apply the concept of proton mobility in order to better define the water-related dynamic aspects of freeze-dried fruits. Different water mobility populations were defined through ^{1}H NMR transversal relaxation times, obtained after the application of several pulses sequences. The water content limits at which proton populations with different mobility appeared, allowed a more complete and precise description of water behavior at the different sorption stages than the parameters obtained by the application of sorption mathematical models.

1. Introduction

Water presence and its interactions with other food compounds are important in defining process variables, stability and food quality aspects. The water sorption behavior in fruits is affected by many variables, such as sugar content, ripening, process and storage conditions (Bolin, 1980; Kaya et al., 2002).

Mathematical interpretation of water sorption isotherms has received much attention due to its relationship with food shelf life (Labuza et al., 1970; Labuza, 1980; Simatos and Karel, 1988). Brunauer–Emmett–Teller (BET) (Brunauer et al., 1938) and Guggenheim–Anderson–de Boer (GAB) (Van Den Berg and Bruin, 1981) are models extensively used. BET model applicability is limited to relative vapor pressure (*RVP*) range between 0.1 and 0.5 (Labuza, 1968) while GAB sorption equation has a wider *RVP* ranging from 0.1 up to around 0.9 (Timmermann, 2003).

Some works on the advantage of the generalized D'Arcy & Watt equation (GDW) (D'Arcy and Watt, 1970) application in foods have been published (Furmaniak et al., 2007a,b, 2009). GDW maintains all the considerations of the GAB model, but also assumes that only a proportion of water molecules bound to primary centers of adsorption can act as secondary centers. Also, in some cases one primary center can absorb more than one water molecule (Furmaniak et al., 2009).

The sorption isotherms have been used for stability estimations, and their partitioning into different zones according to the *RVP* value, as proposed by Labuza and coworkers in 1970, had very important practical applications, and has been referenced and reproduced thousands of times (Schmidt, 2004). The limits between the different zones are, however, difficult to define only with the water sorption data.

It has been recognized that the molecular mobility of water and solids is related to kinetic aspects and its analysis has broad applications in food stability predictions (Le Meste et al., 1991). These studies include different materials as starch (Richardson et al., 1987), sucrose and starch systems (Kou et al., 1999), milk protein concentrate (Haque et al., 2010), apples (Hills and Remigereau, 1997), and pintado fish (Pitombo and Lima, 2003). Thus, the dynamic properties play an important role in complementing the information provided by water sorption isotherms and can be employed for establishing the limits between the different sorption zones.

One of the most successful techniques used to prove the dynamic behavior of water in food systems is pulsed NMR (Le Meste et al., 1991; Hills, 1999; Haque et al., 2010). A relationship between NMR relaxation times and *RVP* can thus allow to have a complete scheme of the water behavior in foods (Schmidt, 2004). The limits of the different water sorption stages have been empirically described but are not well defined. Even more, the references to "bound", "monolayer", "multilayer" and "free" water for indicating the different degree and strength of water–solid interactions are questioned (Fennema, 1999). The definition of zones according to proton mobility could give a more appropriated description. Nuclear magnetic resonance (NMR) technique is employed to characterize the mobility of water and solids in food systems (Schmidt,

* Corresponding author. Tel./fax: +54 11 4576 3366.
E-mail address: pilar@di.fcen.uba.ar (M.d.P. Buera).

0260-8774/$ - see front matter © 2013 Published by Elsevier Ltd.
http://dx.doi.org/10.1016/j.jfoodeng.2013.10.029

2004) and could serve as a reference replacing or complementing the water sorption isotherm concept.

The aim of this study was to apply the concept of proton mobility in order to better define the water-related dynamic aspects of freeze-dried fruits.

2. Materials and methods

2.1. Fruits

Fully ripe fresh apple (Granny Smith), melon (Honeydew) and pear (Packam's Triumph) were obtained from the local market and stored at 4 °C prior to experimentation. The fruits were washed, peeled and were cut transversally into cylinders (2.5 cm diameter and 0.5 cm thickness). The cut material was immediately frozen with liquid nitrogen and stored at −20 °C.

2.2. Materials preparation

Previously frozen fruit cylinders were taken from the −20 °C storage were covered with liquid nitrogen before freeze-drying. A freeze-drier (ALPHA 1–4 LD2 Martin Christ Gefriertrocknungsanlagen GMB, Germany) was used. The freeze-drier was operated at −55 °C, at a chamber pressure of 4 Pa, and the process lasted 48 h. After freeze-drying, samples were humidified at 25 °C for 14 days over saturated salt solutions in vacuum desiccators. Saturated salt solutions of lithium chloride (LiCl), potassium acetate (CH_3CO_2K), magnesium chloride ($MgCl_2$), potassium carbonate (K_2CO_3), magnesium nitrate ($MgNO_3$), sodium chloride (NaCl), and potassium chloride (KCl) were used for 0.11, 0.22, 0.33, 0.43, 0.52, 0.75 and 0.84 *RVP*, respectively (Greenspan, 1977). The selected equilibration time was based on several experiments in different fruits, and the equilibrium was confirmed at the end of the humidification time by measuring the a_w values of the samples using a dew-point water activity meter Aqualab Series 3 (Decagon Devices, Pullman, WA, USA).

2.3. Sugar content

Approximately 1 g of freeze-dried fruit was suspended in 10 mL of ethanol (80%) by mechanical stirring. The resulting suspensions were maintained at 4 °C overnight. Sugar analysis was performed by HPLC (Kontron Eching Germany) isocratically, employing a Thermo Hypersil Amino column (5 μm, 250 mm × 4.6 mm) and a refractive index detector. Acetonitrile:water mixture (70:30) was employed as the mobile phase. An average value of two replicates was reported along with the standard deviation.

2.4. Water content

The water content (wc) of the previously humidified fruits was determined gravimetrically by difference in weight before and after vacuum drying over magnesium perchlorate at 80 °C for 48 h (Agudelo-Laverde et al., 2011), and it was expressed as g H_2O/100 g solids. An average value of at least two replicates was reported along with the standard deviation.

2.5. Mathematic models

The mathematical form of the GAB model is:

$$M = \frac{m_o CKRVP}{(1 - KRVP)(1 - KRVP + CKRVP)}$$

where m_o is the monolayer value (hydration water content), C is the kinetic constant related to the sorption in the first layer, K is the kinetic constant related to multilayer sorption. M is the water content at each *RVP*.

The mathematical form of the GDW model is:

$$M = \frac{M_e KRVP}{(1 + KRVP)} \times \frac{1 - k(1 - w)RVP}{1 - kRVP}$$

where M_e is the maximum sorption value on primary centers, K and k are the kinetic constants related with sorption on primary and secondary centers, and w is the parameter that determines the ratio of molecules bonded to primary centers and converted into the secondary ones. M is the water content at each *RVP*.

The experimental values were mathematically described by GAB and GDW equations by nonlinear regression analysis minimizing the root mean square deviation, through GraphPad Prism 5 software.

2.6. Thermal transitions

Glass transitions were determined by differential scanning calorimetry (DSC; onset values) using a DSC 822e Mettler Toledo calorimeter (Schwerzenbach, Switzerland). The instrument was calibrated with indium (156.6 °C), lead (327.5 °C), zinc (419.6 °C), and water (0 °C). All measurements were performed at a heating rate of 10 °C/min. Hermetically sealed 40 mL medium pressure aluminum pans were used, (an empty pan served as a reference). Thermograms were evaluated using Mettler Stare program.

2.7. Proton mobility

Transversal or spin–spin relaxation times (T_2) were measured by time resolved proton nuclear magnetic resonance (^{1}H NMR) in a Bruker Minispec mq20 (Bruker Biospin Gmbh, Rheinstetten, Germany) with a 0.47 T magnetic field operating at a resonance frequency of 20 MHz. Humidified fruits were removed from the desiccators placed into 10 mm diameter glass tubes and returned to the desiccators for additional 24 h prior to analysis. All determinations were performed in triplicate at 25 °C. The average and standard deviation are reported.

Proton populations of different mobility were measured using the following three methods.

2.7.1. Measurements using a single pulse method

The spin–spin relaxation time (T_2) associated with the fast relaxing protons (related to the protons of the solid matrix and to the water molecules interacting tightly with solids) was measured using a free induction decay analysis (FID) after a single 90° pulse (Schmidt, 2004). The following settings were used: scans = 4, recycle delay = 2 s, gain = 68 dB and number of points = 100. The decay envelopes were fitted to mono-exponential behavior with the following equation:

$$I = A\exp(-t/T_{2-\mathrm{FID}})$$

where I represents the protons' signal intensity, $T_{2\text{-FID}}$ corresponds to the relaxation time of protons in the polymeric chains of the material and of tightly bound water and A is a constant. Since no 180° refocus pulse was used in the experiments, the spin–spin relaxation time constants are apparent relaxation time constants, i.e., T^*_{2-FID}. However for solid materials (like ours), we can consider that the intrinsic $T_{2\text{-FID}}$ is very close to the T^*_{2-FID} as reported previously by Fullerton and Cameron (1988). Therefore, $T_{2\text{-FID}}$ was used for convenience. Dehydrated fruits humidified between 0.11 and 0.84 *RVP* were analyzed using this method. The device was calibrated using three certified standards composed of plastics in oil, provided by Bruker.

2.7.2. Measurements using echo spin sequences

2.7.2.1. Hahn spin-echo sequence. It consists of a $(90° - \tau - 180°)$ sequence (Hahn, 1950). This method is associated with slow relaxing protons (related to the populations of water molecules displaying less interaction with solids); the more mobile protons could not be analyzed using this sequence due to diffusion problems during measurement at long times, caused by inhomogeneities in the magnetic field. Dehydrated fruits humidified between 0.11 and 0.84 *RVP* were analyzed using this sequence. The following settings were used: scans = 4, recycle delay = 1.5 s, gain = 75 dB, number of points = 20, time for decay curve display = 2 s and interpulse (τ) range of 0.001–2 ms. The interpulse range was selected in order to record the complete relaxation of the signal. No phase cycling was used. A polyvinylpyrrolidone (PVP of 58,000 Da) system equilibrated at 0.52 *RVP* was used for the automatic update of the equipment which tunes the pulse duration, detection angles, gain and magnetic field homogeneity.

2.7.2.2. CPMG sequence. The method consists of a $(90^{\circ}_{x} - \tau - (180^{\circ}_{y} - \tau - \text{echo} - \tau)_{n}$ sequence (Carr and Purcell, 1954; Meiboom and Gill, 1958), with the following setting: $\tau = 1$, scans = 4, number points = 200, gain = 75 dB; phase cycling was used. This method is associated with very slow relaxing protons (related to the more mobile populations of water molecules, having little interaction with the solid components). In this case, the mobile protons could be analyzed because the use of several 180° pulses reduces the diffusion problems occurring during measurements at long times. The automatic update of the equipment was performed employing a same PVP used in Hahn sequence studies. Since after the CPMG pulse sequence the low mobility protons had already relaxed, this method allows measuring medium/high proton mobility populations, therefore only dehydrated fruits humidified between 0.52 and 0.84 *RVP* were analyzed using this sequence.

2.7.2.3. Fitting of the magnetization decay. For measurements after Hahn and CPMG pulse sequences, the decay envelopes were fitted to bi-exponential behavior with the following equation:

$$I = A_1 \exp(-t/T_{2-1}) + A_2 \exp(-t/T_{2-2})$$

where I represents the NMR signal intensity at time t. The relaxation time T_{2-1} corresponds to the protons in the less mobile water fraction for each sequence employed. A_1 is proportional to the number of protons in the T_{2-1} state. The relaxation time T_{2-2} corresponds to the more mobile water fraction. A_2 is proportional to the number of protons in the T_{2-2} state.

3. Results and discussion

The sugar composition and T_g values after freeze-drying of apple, melon and pear is shown in Table 1, the sugar proportion which is in agreement with previous reported values (Tóth-Markus et al., 2011; Cohen et al., 2012). All the samples presented high proportion of sugars, in a range between 76% and 87% on total dry solids basis. It is important to note that pear shows the highest fructose content, and the lowest sucrose proportion, while melon presented the lowest fructose concentration and higher glucose proportion. The T_g data were in agreement to those reported for apple and pear (Khalloufi and Ratti, 2003). Similar water contents were reported for apple (Moraga et al., 2011; Acevedo et al., 2008), and pear (Guiné and Castro, 2002).

Table 1
Sugar composition and water content (expressed in g/100 g dry solids) and T_g values of the studied fruits after freeze-drying. The average and the corresponding standard deviations are reported.

Sample	Glucose	Fructose	Sucrose	T_g (°C)	wc
Apple	17.1 ± 0.6	33.3 ± 0.9	25.8 ± 1.0	−7.1 ± 0.5	4.7 ± 0.01
Melon	36.5 ± 1.2	19.1 ± 0.7	23.4 ± 0.7	14.4 ± 0.6	4.6 ± 0.13
Pear	18.3 ± 0.5	57.5 ± 1.7	10.9 ± 0.3	−11.4 ± 0.5	6.3 ± 0.1

3.1. Water sorption isotherms

During primary drying in the freeze-drying process, the cellular spaces left by ice crystal sublimation are replaced by air. The cooling rate and final freezing temperatures determine the number and size of ice crystals generated in intra and extracellular spaces. In consequence, after freeze-drying, a matrix with different water sorption characteristics is obtained, according to the freezing conditions. Fast freezing rates, as those employed in present work generate a high amount of small ice crystals leading to a very tortuous dry matrix as will be discussed later (Delgado and Rubiolo, 2005).

It is known that the use of mathematical models in fitting of sorption water isotherms, are appropriate only for amorphous materials (Harnkarnsujarit and Charoenrein, 2011). The DSC thermograms of the studied fruits, performed in temperature ranges from −100 up to 100 °C, did not show any sign of sugar crystallization (Agudelo-Laverde et al., 2011). Accordingly, the corresponding deltaCp values obtained increased as increasing *RVP*, as expected in supercooled systems (Silalai and Roos, 2010). The lack of crystallizalization in multi-sugar systems has been previously reported, since the presence of different sugars has an inhibitory effect on each other's crystallization (Schebor et al., 2002; Leinen and Labuza, 2006). Thus, considering that the material remained supercooled, without any sign of sugar crystallization, it was possible to apply the GAB and GDW models.

The GAB model was employed to fit the experimental data of water sorption isotherms at 25 °C of freeze-dried apple, melon and pear (Fig. 1). All the water sorption curves showed a sigmoidal shape, which is typical of biological products and food components. According to Brunauer et al. (1940) classification, the resulting curves corresponded to type II. GAB equation is extensively employed to describe water sorption in food matrices, because of the wide range of relative vapor pressures of this model applicability (Timmermann, 2003). In Table 2 the fitting parameters of the GAB equation are summarized for all the studied fruits. Determination coefficients (R^2) showed variations between 0.985 and 0.987.

Water content hydration limit value (m_o, or "monolayer value" as frequently labeled), which corresponds to the first sorption stage described by GAB equation, was slightly higher for pear than for the other studied fruits. The differences in m_o values between fruits could be due to their different sugars proportions (Table 1). Pear is rich in fructose, which is the most hygroscopic sugar and this can explain the highest m_o value obtained for pear isotherm (Pancoast and Junk, 1980).

The obtained values for k_{GAB} were close to, but less than 1, typical of food products (Timmermann, 2003) and in agreement with previously reported by Moraga et al. (2011) values for apple (m_o = 8.6 g H_2O/100 g solids, k_{GAB} = 1.). This constant represents the difference between standard chemical potential of molecules in intermediate mobility zone (second sorption layer), and pure water (Viganó et al., 2012; Tolaba et al., 2004).

The third water sorption stage corresponds to the water molecules with high mobility and its location in the sorption isotherm is very important because it represents the relative vapor pressure limit at which water can dissolve solutes, it is easy to freeze and it is available for reactant mobilization and microbial growth (Labuza et al., 1970; Simatos and Karel, 1988). These phenomena are manifested on curvature changes of the water sorption isotherm. One way to identify the isotherm inflexion point in the high *RVP* range (D_G) is applying the linearization of the GAB equation proposed by Timmermann and Chirife (1991). By this linearization, at initial

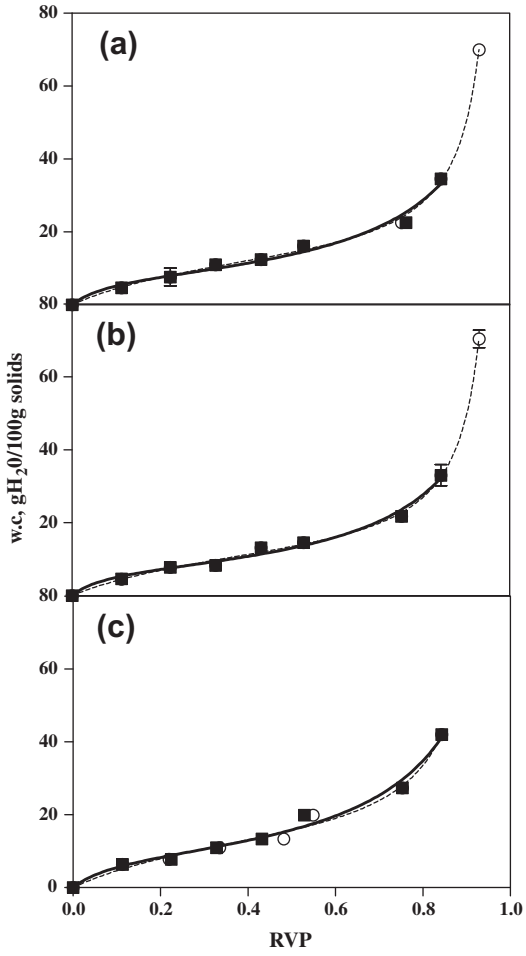

Fig. 1. Water sorption isotherms at 25 °C: experimental points for apple (a), melon (b) and pear (c), and the corresponding GAB (solid symbols and line) and GDW (open symbols and dashed line) fitting. The standard deviations are plotted in the figures.

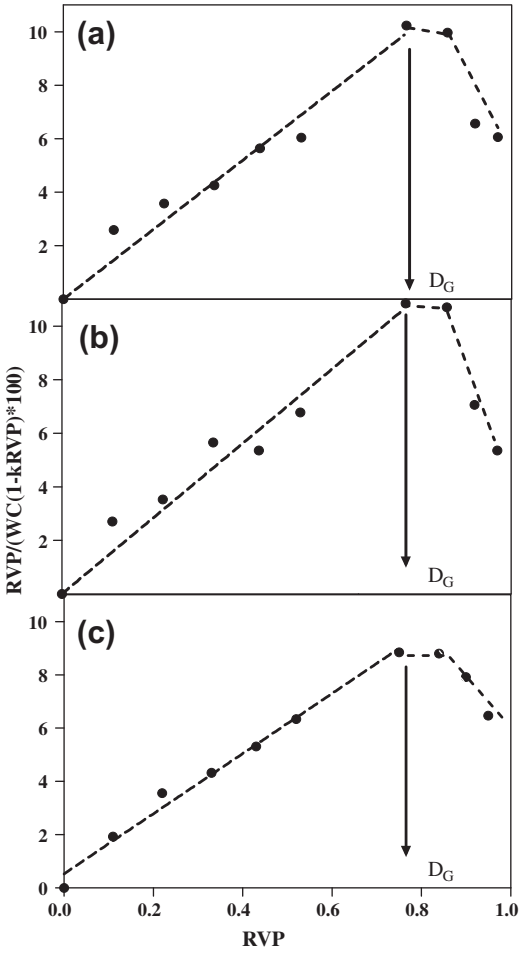

Fig. 2. Linearization of the GAB equation for apple (a), melon (b) and pear (c) at 25 °C.

Table 2
Fitting parameters of the GAB equation for water sorption isotherms at 25 °C. Water content hydration limit value (m_o) is expressed in g H_2O/100 g solids. The average and the standard deviations are reported.

Parameters	Apple	Melon	Pear
m_o	8.3 ± 0.6	8 ± 1	9.4 ± 0.4
k_{GAB}	0.89 ± 0.02	0.91 ± 0.04	0.92 ± 0.01
C	13 ± 6	15 ± 9	11 ± 9
R^2	0.987	0.986	0.985

sorption stages there is a linear relationship between the plotted variables. When the third sorption stage starts, it is possible to detect an important curvature deflection. Linearization of the GAB equation was applied to experimental data of apple (a), melon (b) and pear (c) at 25 °C (Fig. 2).

In all of the studied cases a linear trend was observed until a relative vapor pressure value higher than 0.75 is reached. After 0.75 *RVP*, the experimental data show a deflection which indicates the change of the physical state of the adsorbed water. Adamson (1963) associated the strong increase of water sorption at high *RVP* with capillary condensation.

D'Arcy and Watt (1970) generalized model was also employed to fit the experimental data of water sorption isotherms at 25 °C (Fig. 1). This model has been previously used to describe water sorption isotherms of different food products as marjoram, dill, garlic, milk powered, coffee (Furmaniak et al., 2007a, 2009) and pineapple (Furmaniak et al., 2007b). When each one of the water molecules absorbed in primary sites, is converted to a secondary sorption site, the GDW model is reduced to GAB model. Table 3 shows GDW fitting parameters of water sorption isotherms at 25 °C of freeze-dried apple, melon and pear.

Fitting experimental data of water sorption isotherms by using GDW equation was adequate for all the studied fruits, with correlation coefficients (R^2) ranging between 0.988 and 0.995. GDW equilibrium moisture content values (M_e) were similar for all the studied fruits, and higher than those obtained for m_o by the GAB model (Table 2). This general trend was observed for sugar systems (Furmaniak et al., 2007b, 2009).

Sorption kinetic constants for the primary (K_{GDW}) and secondary sites (k_{GDW}) showed the same behavior in all the studied samples. K_{GDW} presented values higher than one, as corresponds to type II

Table 3
Fitting parameters of the GDW equation for water sorption isotherms at 25 °C. Water content hydration limit value (M_e) is expressed in g H_2O/100 g solids. The average and the standard deviations are reported.

Parameters	Apple	Melon	Pear
M_e	19 ± 1	18 ± 1	21 ± 1
K_{GDW}	2.8 ± 0.5	2.7 ± 0.4	2.7 ± 0.6
k_{GDW}	1.0 ± 0.2	1.0 ± 0.3	1.0 ± 0.6
w	0.26 ± 0.09	0.3 ± 0.1	0.28 ± 0.08
R^2	0.995	0.995	0.988

isotherms of highly hygroscopic materials, while when this variable is lower than 1 the sorption isotherms are classified as type III. No significant differences were observed in the k_{GDW} of the different fruits, which were close to 1. The obtained values indicate that the kinetics of water sorption (both on primary and secondary sites) is similar for the studied materials.

The obtained w values were lower than unit (around 0.3) in all the analyzed fruits, which indicates that only a small ratio (25–30%) of water molecules adsorbed in primary sites were converted into secondary sorption centers. This ratio could be related with the high freezing rate used previous to the freeze-drying process, which produced small pores in the samples structure and high tortuosity, and then, an impediment to create secondary sorption sites. In this way, GDW model allows to establish a relationship with the material structure.

Furmaniak et al. (2011) reported that w values are equal or close to zero for type I isotherms, while this parameter shows values higher than zero for type II and III isotherms.

M_e and w values reported here are in agreement with those reported by Furmaniak et al. (2007b) for pineapple (M_e = 18.57, w = 0.5).

3.2. Proton mobility concept employed to establish the different water sorption zones

Hills (1999) have found a linear correlation between $1/T_2$ and (1−*RVP*) by empirically relating simplified thermodynamic relationships with NMR relaxation times. In Fig. 3 the inverse NMR relaxation times (T_2) values were plotted as a function of (1−*RVP*) for apple (a), melon (b) and pear (c). Relaxation times data shown in Fig. 3 were obtained with different pulse sequences (single 90° pulse, or combined Hahn and CPMG sequences) in order to represent the different proton populations, according to their mobility, in the same sample. The pulse sequence was selected according to the water mobility and the inter-pulse range was selected in order to record the complete relaxation of the signal. Other authors have obtained the relationship between T_2 and *RVP*, determining the relaxation times by applying only CPMG sequence with different inter-pulse times (Hills, 1999; Schmidt, 2004).

Due to the large differences among the magnitude of the relaxation times, the low proton mobility regions (Fig. 3) were analyzed separately from the high proton mobility regions (insets in Fig. 3). Both in the low (high (1−*RVP*) values) and in the high proton mobility regions (low (1−*RVP*) values), $1/T_2$ remained almost constant up to a certain *RVP* value. Above these points a linear increase in $1/T_2$ was observed.

In the low proton mobility regions (insets in Fig. 3) the points at which the linear increase between $1/T_2$ and (1−*RVP*) were observed at *RVP* 0.33. These points represent the *RVP* at which the second proton population appeared after the Hahn pulses sequence is applied, and are indicated in the plots as D_H.

For the high mobility region (Fig. 3) the deviation points were coincident with the D_G value obtained in GAB linearization plot (Fig. 2).

Fig. 4 shows the logarithmic relaxation times (different symbols) and relative vapor pressures plotted as a function of water content (wc) for apple (a), melon (b), and pear (c). The solid curves correspond to the fitting of the GDW model to the water sorption isotherms, and the vertical lines inserted in the graph identify the wc values at which a new proton population, with different mobility, appeared when employing the Hahn or CPMG pulse sequences. The characteristic points indicated in Fig. 4 are m_o and M_e that represent hydration water contents determined by GAB and GDW equation, respectively; D_G, the deflection points obtained from GAB linearization (or the deviation from linearity between $1/T_2$ versus (1−*RVP*); and D_H the point at which $1/T_2$ establishes a linear dependence with (1−*RVP*) in the low mobility region (Fig. 4).

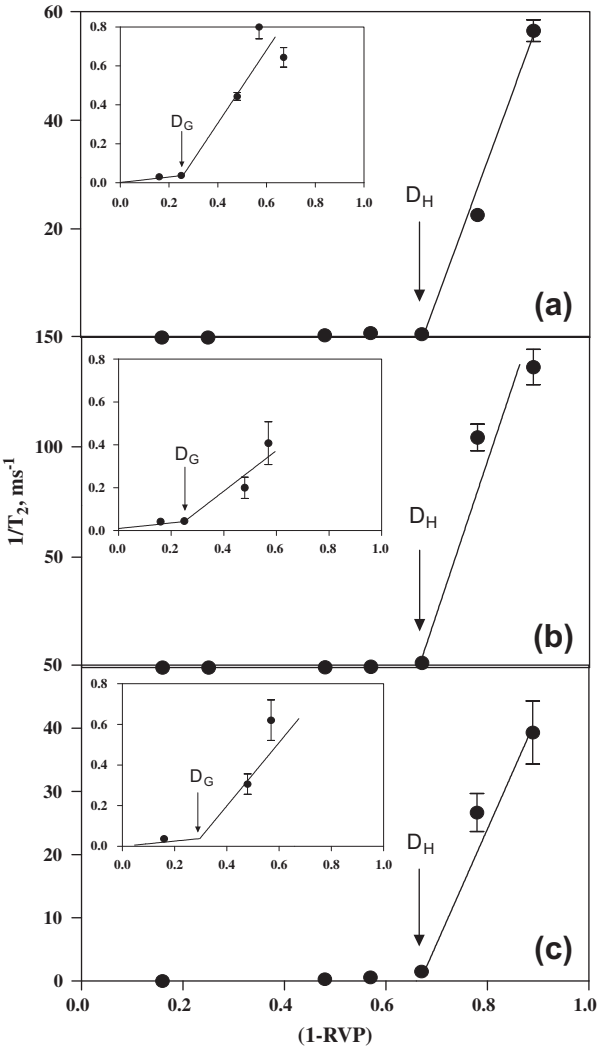

Fig. 3. Relationship between the inverse of the transverse relaxation time ($1/T_2$) and the relative vapor pressure (1−*RVP*) for apple (a), melon (b) and pear (c) for low (correspond to T_2 values determined by single 90° pulse) and high (insets) proton mobility regions (correspond to T_2 values determined by combined Hahn and CPMG sequences).

In this way, three sorption stages could be clearly identified by combining both thermodynamic concepts (water sorption data) and the complementary dynamic relaxations (determined by ^{1}H NMR). In the first stage (I) it was possible to identify only one proton population analyzed after a single 90° pulse or after the Hahn pulse sequence, and is characterized by $\log(1/T_2)$ values between −2 and −1.3, corresponding to relaxation times between 10 and 50 μs in all the studied fruits. These relaxation times are characteristic of protons of sample solids and consequently to water protons strongly associated to the solid components. The upper limit of the stage (I) was defined by the appearance of a second proton population after the Hahn pulse sequence (indicated by a grey circle). It is to be noted that the "monolayer value" obtained through GAB equation was located within the values of stage (I).

The second water sorption stage (II), can be defined from the appearance of the second (slow relaxing) proton population after the Hahn pulse sequence, which corresponds to protons of water molecules with intermediate mobility, with relaxation times ranging from about 1 up to 5 ms. It is important to note that this water content was coincident with the deflection point D_H observed in

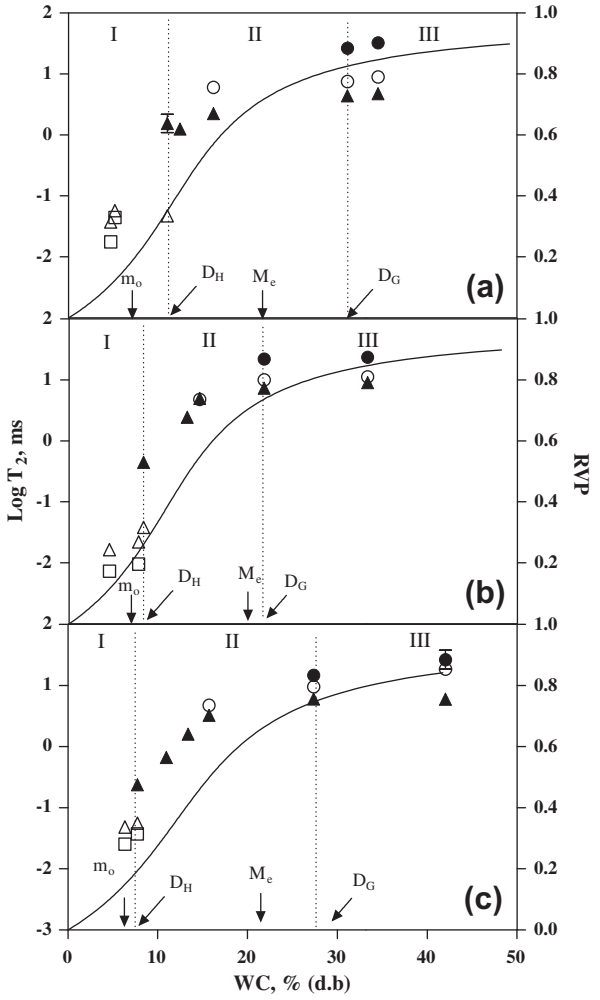

Fig. 4. LogT_2 determined by a single 90° pulse (□) by Hahn pulse sequence (△, ▲) and by CPMG pulse sequences (○, ●) as a function of wc for apple (a), melon (b) and pear (c). The solid curves correspond to the fitting of the GDW model to the water sorption isotherms (*RVP* in the right axis). The vertical lines identify the wc values at which a new proton population appeared when employing the Hahn (▲) or CPMG (●) pulse sequences. m_o and M_e correspond to the hydration limits obtained by GAB and GDW equations, respectively. D_G, deflection points were obtained from GAB linearization; and D_H are the points at which $1/T_2$ establishes a linear dependence with (1−*RVP*) in the low mobility region.

Fig. 3. It can be observed that the M_e values of GDW equation were positioned within the limits of stage II.

The upper wc limit of the sorption stage II, or "polymolecular sorption" zone (Furmaniak et al., 2009) is coincident with the appearance of a second (slow relaxing) proton population after CPMG pulse sequence (indicated by a grey square). Interestingly, this water content was concomitant with the deflection point of the GAB linearization, D_G (Fig. 2) and with the deflection point observed in Fig. 3. Also, at higher water contents than this point, frozen water could be detected by DSC after cooling the samples at −90 °C (data not shown). The third water sorption stage represents the high mobility water molecules, at which the diffusional phenomena become important (in the studied fruit samples it corresponds to water contents higher than 30% d.b.).

Only the samples at water contents corresponding to the second and third water sorption isotherm stages (Fennema, 1996) showed FID signals after application of CPMG pulse sequences, since the protons with lower mobility had already relaxed before the end of the CPMG pulse sequence. Thus, the CPMG sequence can be employed only in samples of water contents corresponding to stages II or III.

It is to be noted that, while the sorption parameters and the limit between the first and second sorption stages were similar for all the studied materials, the boundary between the second and third sorption stages can show differences, as can be seen in Fig. 4. As discussed before, the point at which the linearization of the GAB model deflects, which is coincident with the limit between sorption stages II and III, occurs at the same *RVP* value (0.75) for all the fruits (Fig. 2). However, due to the different sugars and biopolymer composition, the water content at which the defection was observed was different for each material. In the case of pear and apple, which have intermediate content of total sugars but high proportion of the most soluble sugars (fructose and sucrose, as shown in Table 1) the third zone begins at about 30% wc. The lowest limit between the second and third stage was observed for melon samples, which have the highest content of glucose and the lowest proportion of the most soluble sugars.

4. Conclusions

^{1}H NMR transversal relaxation times, obtained by several methods (single 90° pulse, Hahn or CPMG sequences), can be applied for an appropriate definition of the different water mobility populations, related to the water sorption stages.

The water content limits at which discontinuities in the proton populations (i.e., the appearance of proton populations with different mobility) were observed, allowed a more complete description of water behavior at the different sorption stages than the parameters obtained by the application of sorption mathematical models. It is to be noted, however, that the points at which a second proton population appeared, determined through transversal relaxation times by CPMG pulse sequence were coincident with the deflection in the GAB linearization plot indicting the highest water mobility population.

The water hydration limits calculated through GDW (M_e) were higher than those obtained by GAB model (m_o), and both values were positioned in zones with different mobility, as defined by the proton relaxation times. While m_o was in the lowest mobility stage, M_e was located in the intermediate water mobility zone. However, they do not provide a meaningful information regarding the molecular mobility and other kinetic aspects, which are key factors defining food stability. On the other side, ^{1}H NMR relaxation times were in agreement with the compositional aspects regarding sugar solubility and molecular mobility, offering a direct relationship with the dynamic aspects of the materials.

Acknowledgments

The authors acknowledge financial support from UBACYT 20020100100397, ANPCYT (PICT-2008 0928) and CONICET (PIP 11220090100846).

References

Acevedo, N.C., Briones, V., Buera, M.P., Aguilera, J.M., 2008. Microstructure affects the rate of chemical, physical and color changes during storage of dried apple. Journal of Food Engineering 58 (2), 222–231.
Adamson, A.W., 1963. Physical Chemistry of Surfaces. Wiley, Wiley.
Agudelo-Laverde, L.M., Acevedo, N., Schebor, C., Buera, M.P., 2011. Integrated approach for interpreting browning rate dependence with relative humidity in dehydrated fruits. LWT Food Science and Technology 44, 963–968.
Bolin, H.R., 1980. Relation of moisture to water activity in prunes and raisins. Journal of Food Science 45, 1190–1192.
Brunauer, S., Emmet, P., Teller, E., 1938. Adsorption of gases in multimolecular layers. Journal of the American Chemical Society 60, 309–319.
Brunauer, S., Demming, L., Demming, W., Teller, E., 1940. On a theory of the Van der Waals adsorption of gases. Journal of the American Chemical Society 62, 1723–1732.
Carr, H.Y., Purcell, E.M., 1954. Effects of diffusion on free precession in Nuclear Magnetic Resonance Experiments. Physical Review 94, 630–638.

Cohen, S., Tzuri, G., Harel-Beja, R., Itkin, M., Portnoy, V., Sa'ar, U., Lev, S., Yeselson, L., Petrikov, M., Rogachev, I., Aharoni, A., Ophir, R., Tadmor, Y., 2012. Co-mapping studies of QTLs for fruit acidity and candidate genes of organic acid metabolism and proton transport in sweet melon (*Cucumis melo* L.). Theoretical and Applied Genetics 125, 343–353.

D'Arcy, R.L., Watt, I.C., 1970. Analysis of sorption isotherms of nonhomogeneous sorbents. Transaction Faraday Society 66, 1236–1240.

Delgado, A., Rubiolo, A., 2005. Microstructural changes in strawberry after freezing and thawing processes. LWT Food Science and Technology 38, 135–142.

Fennema, O., 1996. Water and ice. In: Damodaran, S., Parkin, K., Fennema, O. (Eds.), Food Chemistry. CRC Press, New York.

Fennema, O., 1999. Water: the star of biomanipulators obscured in a cloud of superficial familiarity. In: Roos, Y.H., Leslie, R.B., Lillford, P.J. (Eds.), Water Management in the Design and Distribution of Quality Foods: ISOPOW 7. Technomic Publishing Company, Inc., Pennsylvania, USA.

Fullerton, G.D., Cameron, I.L., 1988. Relaxation of biological tissues. In: Wehrli, F.W. (Ed.), Biomedical Magnetic Resonance Imaging. VCH Publishers, New York, pp. 115–155.

Furmaniak, S., Terzyk, A.P., Gauden, P.A., 2007a. The general mechanism of water sorption on foodstuffs – importance of the multitemperature fitting of data and the hierarchy of models. Journal of Food Engineering 82, 528–535.

Furmaniak, S., Terzyk, A.P., Gauden, P.A., Rychlicki, G., 2007b. Applicability of the generalised D'Arcy and Watt model to description of water sorption on pineapple and other foodstuffs. Journal of Food Engineering 79, 718–723.

Furmaniak, S., Terzyk, A.P., Gołembiewski, R., Gauden, P.A., Czepirski, L., 2009. Searching the most optimal model of water sorption on foodstuffs in the whole range of relative humidity. Food Research International 42, 1203–1214.

Furmaniak, S., Terzyk, A.P., Gauden, P.A., 2011. Some remarks on the classification of water vapor sorption isotherms and Blahovec and Yanniotis isotherm equation. Drying Technology 29, 984–991.

Greenspan, L., 1977. Humidity fixed points of binary saturated aqueous solutions. Journal of Research of the National Institute of Standards and Technology 8, 89–96.

Guiné, R., Castro, J., 2002. Experimental determination and computer fitting of desorption isotherms of *D. joaquina* pears. Institutions of Chemical Engineers 80, 149–154.

Hahn, E.L., 1950. Spin echoes. Physical Review 80 (4), 580–594.

Haque, E., Bhandari, B.R., Gidley, M.J., Deeth, H.C., Moller, S.M., Whittaker, A.K., 2010. Protein conformational modifications and kinetics of water-protein interactions in milk protein concentrate powder upon aging: effect on solubility. Journal of Agricultural and Food Chemistry 58, 7748–7755.

Harnkarnsujarit, N., Charoenrein, S., 2011. Effect of water activity on sugar crystallization and b-carotene stability of freeze-dried mango powder. Journal of Food Engineering 105, 592–598.

Hills, B.P., 1999. NMR studies of water mobility in foods. In: Roos, Y.H., Leslie, R.B., Lillford, P.J. (Eds.), Water Management in the Design and Distribution of Quality Foods: ISOPOW 7. Technomic Publishing Company, Inc., Pennsylvania, USA.

Hills, B.P., Remigereau, B., 1997. NMR studies of changes in subcellular water compartmentation in parenchyma apple tissue during drying and freezing. International Journal of Food Science and Technology 32, 51–61.

Kaya, A., Gogus, F., Maskan, M., 2002. Moisture sorption isotherms of grape pestil and foamed grape pestil. Nahrung/Food 46, 73–75.

Khalloufi, S., Ratti, C., 2003. Quality deterioration of freeze-dried foods as explained by their glass transition temperature and internal structure. Journal of Food Science 68 (3), 892–903.

Kou, Y., Molitor, P.F., Schmidt, S.J., 1999. Mobility and stability characterization of model food systems using NMR, DSC, and conidia germination techniques. Journal of Food Science 64 (6), 950–959.

Labuza, T., 1968. Sorption phenomena in foods. Food Technology 24, 543–550.

Labuza, T.P., 1980. Enthalpy/entropy compensation in food reactions. Food Technology 2, 67–77.

Labuza, T., Tannenbaum, S., Karel, M., 1970. Water content and stability of low-moisture and intermediate moisture foods. Food Technology 24 (12), 543–550.

Le Meste, M., Voilley, A., Colas, B., 1991. Influence of water on the mobility of small molecules dispersed in a polymeric system. In: Levine, H., Slade, L. (Eds.), Water Relationship in Foods Advances in the 1980s and Trend for the 1990s, New York, pp. 123–138.

Leinen, K.M., Labuza, T.P., 2006. Crystallization inhibition of an amorphous sucrose system using raffinose. Journal of Zhejiang University Science B 7 (2), 85–89.

Meiboom, S., Gill, D., 1958. Modified spin-echo method for measuring nuclear magnetic relaxation times. Review of Scientific Instruments 29, 688–691.

Moraga, G., Talens, P., Moraga, M.J., Martínez-Navarrete, N., 2011. Implication of water activity and glass transition on the mechanical and optical properties of freeze-dried apple and banana slices. Journal of Food Engineering 106, 212–219.

Pancoast, H.M., Junk, W., 1980. Handbook of Sugars. AVI Pub. Co. Westport, Conn. (USA), p. 598.

Pitombo, R.N.M., Lima, G.A.M.R., 2003. Nuclear magnetic resonance and water activity in measuring the water mobility in Pintado (*Pseudoplatystoma corruscans*) fish. Journal of Food Engineering 58, 59–66.

Richardson, S.J., Baianu, I.C., Steinberg, M.P., 1987. Mobility of water in starch powders determined by nuclear magnetic resonance. Starch 39 (6), 198–203.

Schebor, C., Chirife, J., Buera, M.P., 2002. Amorphous-crystalline transitions and water sorption behavior in raffinose systems. In: Bottini, S., Pereda, S. (Eds.), Proceedings IV Iberoamerican Conference on Phase Equilibria and Fluid Properties for Process Design (in CD), EQ 98, p. 10.

Schmidt, S.J., 2004. Water and solid mobility in foods. In: Taylor, S.L. (Ed.), Advance in Food and, Nutrition Research, vol. 48. Nebraska.

Silalai, N., Roos, Y.H., 2010. Roles of water and solids composition in the control of glass transition and stickiness of milk powders. Journal of Food Science 75 (5), 285–296.

Simatos, D., Karel, M., 1988. Characterization of the condition of water in foods: physico-chemical aspects. In: Seow, C. (Ed.), Food Preservation by Moisture Control, vol. 24–30. New York.

Timmermann, E., 2003. Multilayer sorption parameters: BET or GAB values? Colloids and Surfaces 220, 235–260.

Timmermann, E., Chirife, J., 1991. The physical state of water sorbed at high activities in starch in terms of GAB sorption equation. Journal of Food Engineering 13 (3), 171–179.

Tolaba, M.P., Peltzer, M., Enriquez, N., Pollio, M.L., 2004. Grain sorption equilibria of quinoa grains. Journal of Food Engineering 61, 365–371.

Tóth-Markus, M., Bánáti, D., Adányi, N., Boross, F., Konrád-Németh, C., Szabó, Z., Soltész, M., Nyéki, J., 2011. Composition and storage of pear cultivars from Nagykanizsa. International Journal of Horticultural Science 17 (1–2), 63–68.

Van den Berg, C., Bruin, S., 1981. Water activity and its estimation in foods systems: theoretical aspects. In: Rockland, L.B., Stewart, G.F. (Eds.), Water Activity: Influences on Food Quality, New York, pp. 1–61.

Viganó, J., Azuara, E., Telis, V.R.N., Beristain, C.I., Jiménez, M., Telis-Romero, J., 2012. Role of enthalpy and entropy in moisture sorption behavior of pineapple pulp powder produced by different drying methods. Thermochimica Acta 528, 63–71.